Research on Chemical Intermediates (2021) 47:2143–2159
https://doi.org/10.1007/s11164-020-04390-7

Hexamethylenetetramine-based ionic liquid anchored onto the metal–organic framework MIL-101(Cr) as a superior and reusable heterogeneous catalyst for the preparation of hexahydroquinolines

Saleheh Sanaei-Rad[1] · Hakimeh Saeidiroshan[2] · Boshra Mirhosseini-Eshkevari[1] · Mohammad Ali Ghasemzadeh[1]

Received: 30 November 2020 / Accepted: 31 December 2020 / Published online: 11 January 2021

Abstract

Regarding the significance of medicinal and pharmacological sciences, we explored one-pot multicomponent reaction of aromatic aldehydes, aryl amines, malononitrile and dimedone in the presence of HMTA-BAIL@MIL-101 (Cr) as a novel, stable and strong catalyst. The remarkable features of this approach are good to excellent yields (92–98%), short reaction times (10–20 min), low catalyst loading, reusability and stability of the catalyst. The prepared hexamethylenetetramine-based ionic liquid/MIL-101(Cr) composite was identified via FE-SEM, XRD, EDS, TGA, BET and FT-IR techniques.

Keywords Multicomponent reactions · Quinoline derivatives · Metal–organic frameworks · Brønsted acidic ionic liquid · Heterogeneous catalyst

Introduction

Metal–organic frameworks (MOFs) are among coordination polymers with metal nodes connected by organic linkers via robust coordination bonds in 3D net creating hybrid crystalline microporous substances. The MOFs have the main advantage compared to other porous materials, which is their capability at tuning their topology, functionality and pore size by cautiously selecting the inorganic metal centers and organic linkers [1–4]. Hence, such materials are regarded as potential candidates for various applications in several areas, such as gas storage, catalysis and molecular sensing [5–9]. MOFs are used as suitable support for the immobilization of various

✉ Mohammad Ali Ghasemzadeh
ghasemzadeh@qom-iau.ac.ir

[1] Department of Chemistry, Islamic Azad University, Qom Branch, Qom, Iran

[2] Department of Organic Chemistry, Faculty of Chemistry, University of Kashan, Kashan, Iran

materials like ionic liquids (ILs) and catalysts [10–17]. The structure of MOFs can be functionalized through post-synthetic modification (PSM) method with covalent modification of the organic linkers or incorporation of organic molecules at coordinately on metal sites of MOFs structures. Studies have been performed on ILs with various properties such as negligible vapor pressure, adjustable chemical and physical properties, good thermal stability, high catalytic activity as green and novel catalysts [18, 19]. ILs have different applications in different reactions like nitration, alkylation, Michael addition, Diels–Alder, esterification, etc. [20–27]. Multicomponent reactions (MCRs) are one-pot procedures where various accessible components easily have reactions to create a single product [28]. Hence, considerable advantages have been provided over the conventional linear phase synthesis, by decreasing the time, saving energy, raw materials and money, therefore, both environmental and economical benefits are resultant. Quinolines, owing to their pharmacological and lucrative biological features, are utilized as an important group of heterocyclic compounds in the pharmaceutical uses like antimalarial [29], anticancer [30], antibacterial [31], antiproliferative [32] and antistaphylococcal activities [33]. There are several methods reported in the literature for the synthesis of quinoline derivatives which catalyzed by different catalysts such as $Zr(HPO_4)_2$ [34], CECILs [35], Fe_3O_4 [36] and MNP@BSAT@$Cu(OAc)_2$ [37]. Recently, we have reported different synthetic approaches for numerous products utilizing nanocatalysts [38–42].

Herein, we report the use of HMTA-BAIL@MIL-101(Cr) as a novel and efficient Brønsted acidic ionic liquid for the preparation of hexahydroquinoline derivatives through a one-pot four-component reaction of aromatic aldehyde, malononitrile, dimedone and arylamines under solvent-free conditions (Scheme 1).

Experimental

Materials and instrumentation

Chemicals were purchased from the Sigma-Aldrich and Merck in high purity. All of the materials were of commercial reagent grade and were used without further purification. All melting points were uncorrected and were determined in capillary tube on Boetius melting point microscope. ^{1}H NMR and ^{13}C NMR spectra were obtained on Bruker 250 MHz spectrometer with DMSO-d_6 as a solvent and using TMS as

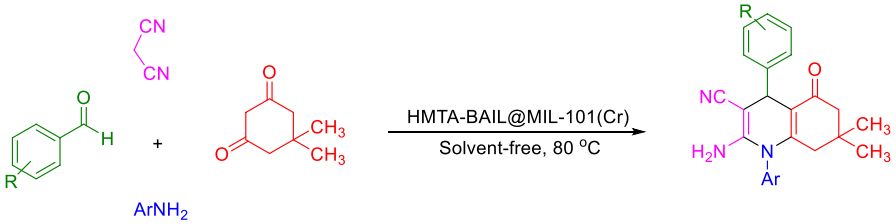

Scheme 1 Synthesis of hexahydroquinoline derivatives using HMTA-BAIL@MIL-101(Cr)

an internal standard. FT-IR spectra were recorded on Magna-IR, spectrometer 550. The elemental analyses (C, H, N) were obtained from a Carlo ERBA Model EA 1108 analyzer. Powder X-ray diffraction (XRD) was carried out on a Philips diffractometer of X'pert Company with monochromatized Cu·Kα radiation ($\lambda = 1.5406$ Å). Microscopic morphology of products was visualized by SEM (LEO 1455VP). The mass spectra were recorded on a Joel D-30 instrument at an ionization potential of 70 eV. The compositional analysis was done by energy-dispersive analysis of X-ray (EDX, Kevex, Delta Class I). Thermogravimetric analysis (TGA) was performed on a Mettler Toledo TGA under argon and heated from room temperature to 825 °C. Nitrogen adsorption–desorption isotherms were measured at 196 °C using a Belsorp mini automatic adsorption instrument after degassing the samples at 150 °C for 5 h. The approximate sample weight was 10 mg in TG experiment with 10 °C/min heating rate.

Preparation of HMTA-BAIL

The synthesis of HMTA-BAIL was done based on the previous literature with a slight modification [43]. A mixture of hexamethylenetetramine (0.01 mol) and 1,4-butane sultone (0.08 mol) in toluene (40 mL) was exposed to magnetic stirring at 80 °C for 72 h. The produced white solid zwitterion (HMTA-BAIL precursor) was filtered out and washed repeatedly by diethyl ether. An ionic liquid was formed through adding a stoichiometric quantity of sulfuric acid to the zwitterion and then stirred the produced admixture at 80 °C for 6 h. Lastly, the BAIL phase was rinsed several times by toluene and diethyl ether for the removal of non-ionic remains, and then dehydrated under vacuum at 110 °C (Scheme 2).

Preparation of MIL-101(Cr)

The preparation of MIL-101(Cr) was performed under hydrothermal conditions based on a previously used procedure with minor modification (Scheme 3) [44]. Briefly, a mixture of $Cr(NO_3)_3.9H_2O$ (5.4 g), terephthalic acid (1.5 g), deionized water (45 mL) and 0.6 mL of hydrofluoric acid (5 mol/L) was sonicated for 10 min. Then, the mixture was transferred to a Teflon-lined stainless steel autoclave for 8 h at 220 °C. Subsequent to cooling down the autoclave to ambient temperature, the reaction mixture

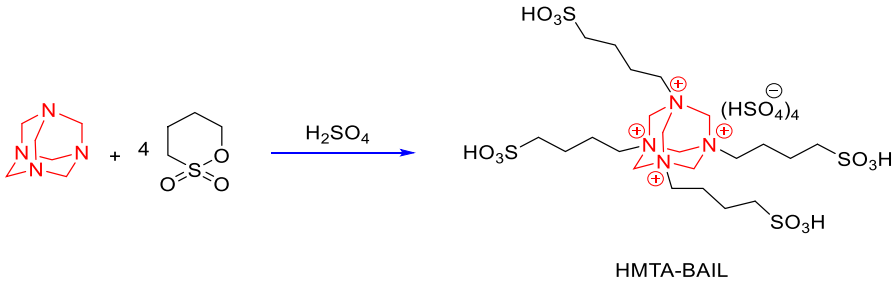

Scheme 2 Synthesis of HMTA-BAIL

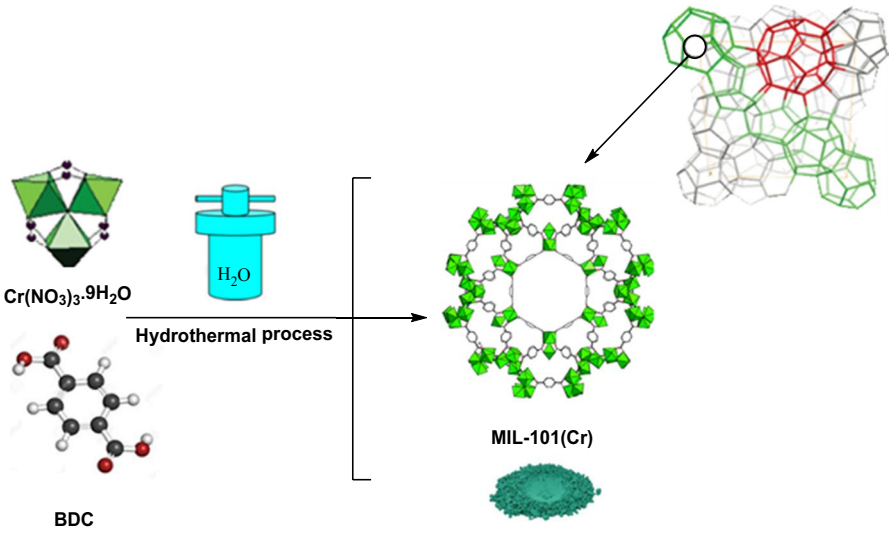

Scheme 3 Preparation of MIL-101(Cr)

was subjected to filtration and washing by distilled water. The resultant solid was dehydrated in an oven at 80 °C nightlong and denoted as crude MIL-101(Cr) crystals.

Preparation of HMTA-BAIL@MIL-101(Cr)

Scheme 4 displays the preparing procedure of the new and vigorous Brønsted acidic ionic liquid functionalized MIL-101(Cr) MOF. In brief, dehydration of MIL-101(Cr) (1.0 g) was done under vacuum at 110 °C for 12 h. A suspension of MIL-101(Cr) in anhydrous toluene (30 mL) was prepared in a round-bottom flask, and hexamethylenetetramine (5 mmol) was added afterward. The reaction mixture was refluxed under stirring at 80 °C for 12 h. To separate the solvent, it was filtrated upon the termination of the reaction, and then washed by toluene to remove the extra hexamethylenetetramine. Thereafter, the product was dissipated in 30 mL of anhydrous toluene. Throughout stirring vigorously, an equal molar ratio 1,4-butane sultone (5 mmol) was incorporated into the solution, followed by refluxing the admixture at 80 °C for 12 h. Finally, the solid was harvested via filtration and dehydrated under vacuum at 110 °C for 3 h. A suspension of the solid was then made in 20 mL of ethanol simultaneously an equivalent amount of concentrated H_2SO_4 (98%) was added dropwise at 50 °C for 24 h. In the end, the catalyst was isolated by filtration and desiccated under vacuum at 50 °C for 12 h.

General procedure for the synthesis of hexahydroquinoline derivatives (5a–5n).

A mixture of aromatic aldehyde (1 mmol), dimedone (1 mmol), aryl amine (1 mmol), dimedone (1 mmol) and HMTA-BAIL@MIL-101(Cr) (0.008 g) was

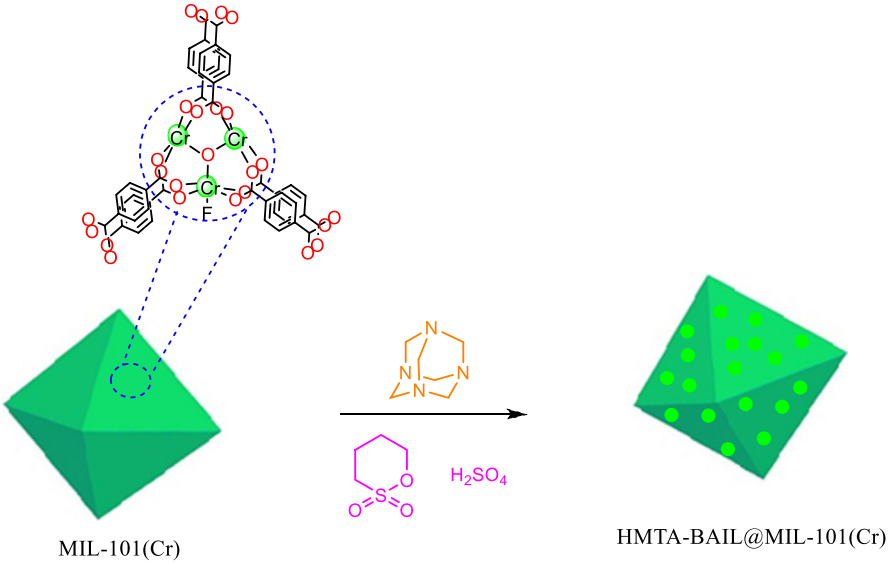

Scheme 4 Preparation of HMTA-BAIL@ MIL-101(Cr)

heated at 80 °C under solvent-free conditions. After completion of the reaction, as monitored with TLC (*n*-hexane:ethyl acetate, 4:1), the reaction mixture was cooled to room temperature, diluted with acetone (10 mL) and stirred for additional 10 min. The catalyst was insoluble in acetone and was separated by simple filtration. Finally, after evaporation of the solvent the crude product was recrystallized from EtOH to produce pure hexahydroquinoline derivatives.

Spectral data of the new products are given below.

2-amino-4-(4-cyanophenyl)-7,7-dimethyl-5-oxo-1-(p-tolyl)-1,4,5,6,7,8 hexahydroquinoline-3-carbonitrile 5d. Yellow solid; m.p. 241–242 °C. IR spectrum ν, cm^{-1}: 3313, 3209, 2958, 2225, 2179, 1635, 1512, 1365, 1223; ^{1}H NMR (250 MHz, DMSO-d_6) δ: 0.84 (s, 3H, CH_3), 0.98 (s, 3H, CH_3), 1.88–1.99 (m, 2H, 2CH), 2.20–2.38 (m, 2H, 2CH), 2.47 (s, 3H, CH_3), 4.48 (s, 1 H, CH), 5.28 (s, 2 H, NH_2), 6.76–7.03 (d, 2H, ArH), 7.29–7.31 (d, 2H, ArH), 7.61–7.77 (m, 4H, ArH); MS (EI) (m/z): 408.20 (M^+); Anal. Calcd. for: $C_{26}H_{24}N_4O$: C 76.45, H 5.92, N 13.72. Found: C 76.58, H 5.89, N 13.65.

2-amino-7,7-dimethyl-4-(4-(methylthio)phenyl)-5-oxo-1-(p-tolyl)-1,4,5,6,7,8-hexahydroquinoline-3-carbonitrile 5e. Yellow solid; m.p. 255–257 °C. IR spectrum ν, cm^{-1}: 3321, 3186, 2954, 2187, 1651, 1522, 1369, 1215; ^{1}H NMR (250 MHz, DMSO-d_6) δ: 0.84 (s, 3H, CH_3), 0.92 (s, 3H, CH_3), 1.77–2.12 (m, 2H, 2CH), 2.19–2.25 (m, 2H, 2CH), 2.44 (s, 3H, CH_3), 2.47 (s, 3H, SCH_3), 4.12 (s, 1 H, CH), 5.33 (s, 2 H, NH_2), 6.78–6.98 (m, 2H, ArH), 7.08–7.19 (m, 6H, ArH); MS (EI) (m/z): 429.19 (M^+); Anal. Calcd. for: $C_{26}H_{27}N_3OS$: C 72.70, H 6.34, N 9.78. Found: C 72.61, H 6.39, N 9.86.

Results and discussion

The structure elucidation of the catalyst

In the initial experiments, the hexamethylenetetramine-based ionic liquid/MIL-(101) Cr composite was characterized by field emission scanning electron microscopy (FE-SEM), Fourier transform infrared spectroscopy (FT-IR), powder X-ray diffraction patterns (XRD), energy-dispersive X-ray (EDX), N_2 adsorption–desorption isotherm (BET) and thermogravimetric analysis (TGA).

SEM analysis was studied to distinguish the particle size and surface morphology of the synthesized HMTA-BAIL@ MIL-101(Cr). FE-SEM micrograph of the as-synthesized MIL-101(Cr) and HMTA-BAIL@MIL-101(Cr) (Fig. 1a and b) representing a characteristic octahedral shape form.

The FT-IR spectra of the BAIL-functionalized MIL-101(Cr) and bare MIL-101 (Cr) nanostructure are represented in Fig. 2. The two sharp peaks around 1385 and 1665 cm^{-1} are equivalent to asymmetric and symmetric vibrations of C=C [45]. Moreover, Cr–O bonds-related peaks appeared at, respectively, 550 and 663 cm^{-1}. The peaks at 1203 cm^{-1} accompanied by a shoulder at 1452 cm^{-1} which is related to the O=S=O asymmetric and symmetric stretching modes, nevertheless, the bands at 1155 cm^{-1} are allocated to the S–O stretching vibrations.

The PXRD (powder X-ray diffraction) patterns of the BAIL-functionalized MIL-101(Cr) substances represent nearly all the main diffraction peaks regarding the pure MIL-101(Cr) and simulated pattern (Fig. 3). Such findings showed that the MIL-101(Cr) materials' crystalline structures were unaffected and remained intact over the BAIL functionalization procedure. The reflection planes equivalent to the Miller indices (201), (311), (440), (402), (333), (531), (606), (753), (666) and (600) are indexed for the MIL-101 consistent with the reported values [44, 46]. It is found that there is a good consistency between the representative peaks of the synthesized HMTA-BAIL@MIL-101 (Cr) materials and MIL-101 (Cr). There is also an agreement between the observations and the one reported in the studies [47].

Figure 4 demonstrates the elemental analysis of MIL-101(Cr) and HMTA-BAIL@MIL-101(Cr) obtained from EDX. The results confirm the existence of C,

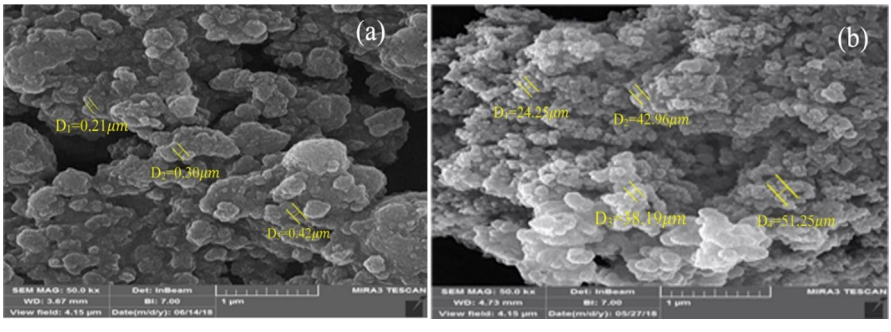

Fig. 1 FE-SEM images of MIL-101(Cr) (**a**) and HMTA-BAIL@MIL-101(Cr) (**b**)

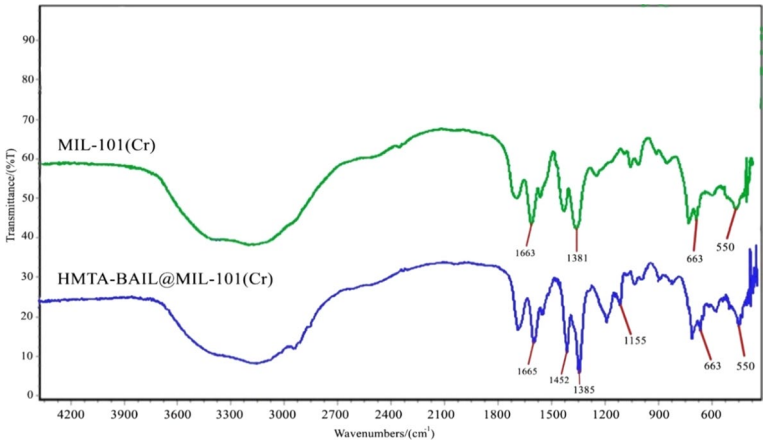

Fig. 2 The FT-IR spectra of MIL-101(Cr) MOF and HMTA-BAIL@ MIL-101(Cr)

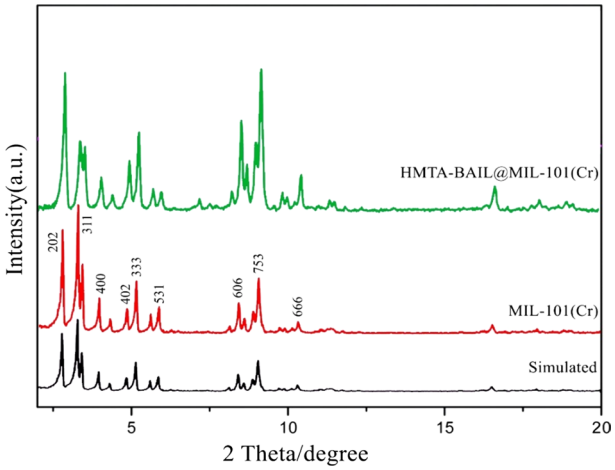

Fig. 3 XRD patterns of MIL-101(Cr) and HMTA-BAIL@MIL-101(Cr)

O, Cr, F and N as the only elementary components of MIL-101(Cr) MOF (Fig. 4a). The purity of HMTA-BAIL@ MIL-101(Cr) was also confirmed by appearance of C, O, Cr, F, N and S as elements in EDX analysis (Fig. 4b).

The N_2 adsorption–desorption isotherm of MIL-101 (Cr) and HMTA-BAIL@ MIL-101 (Cr) is shown in Fig. 5. Measuring pore volume and surface area of HMTA-BAIL@ MIL-101 (Cr) represents their reduction in comparison with pristine MIL-101 (Cr). The pure MIL-100 (Cr) represented an overall pore volume and a BET surface area of 1.42 cm^3/g and 2473 m^2/g; however, HMTA-BAIL@ MIL-101(Cr) represented corresponding values of 1.06 cm^3/g and 1921 m^2/g. The reduced porosity may be related to the pore blockage of MIL-101(Cr) via the BAIL group.

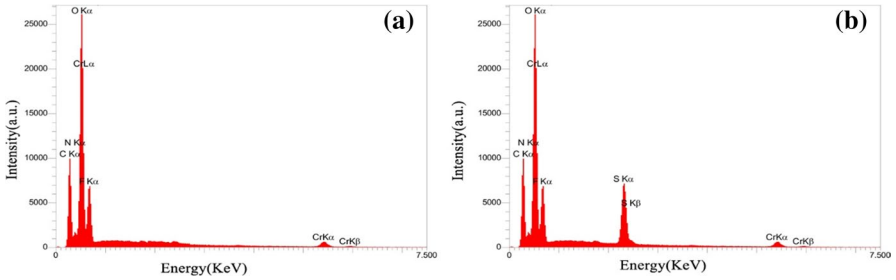

Fig. 4 The EDX spectra of MIL-101(Cr) MOF (**a**) and HMTA-BAIL@MIL-101(Cr) (**b**)

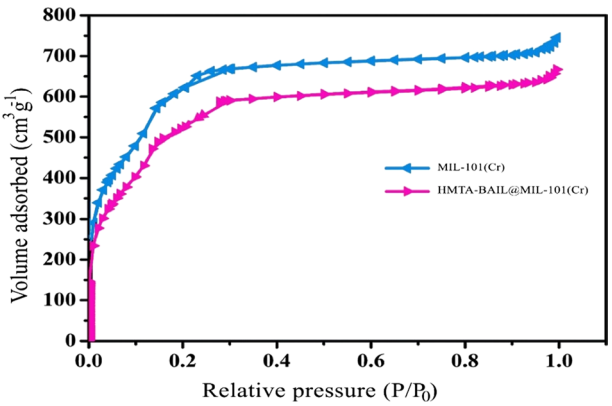

Fig. 5 The N_2 adsorption–desorption isotherms at 77 K of MIL-101(Cr) and HMTA-BAIL@MIL-101(Cr)

The thermogravimetric analysis curves for MIL-101(Cr) and HMTA-BAIL@MIL-101(Cr) show two-step weight losses at < 200 °C and 200 to 400 °C, respectively (Fig. 6). The first weight step appeared at < 200 °C, which was attributed to the loss of solvents from the framework. The subsequent loss at 200–400 °C can be attributed to decomposing the immobilized ionic liquid moieties into the MIL-101(Cr) nanocages, causing the collapse of framework.

Optimization of the reaction conditions

In this research, we report an efficient method for the synthesis of hexahydroquinoline derivatives in high yields via the multicomponent reaction of aromatic aldehydes, malononitrile, dimedone and aryl amines in the presence of HMTA-BAIL@MIL-101(Cr) as an efficient catalyst. To optimize the reaction conditions, the model reaction was performed using 3-nitrobenzaldehyde (1 mmol), malononitrile (1 mmol), dimedone (1 mmol) and aniline (1 mmol) under various conditions. The reaction conditions were optimized based on the solvent, catalyst and different temperatures for the synthesis of hexahydroquinoline **5c** (Scheme 5).

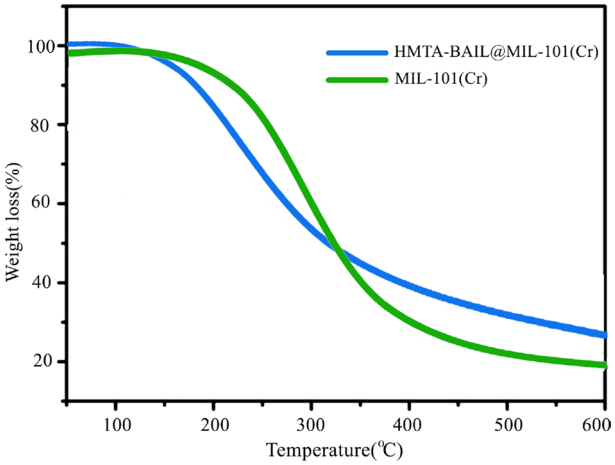

Fig. 6 TGA curves of the MIL-101(Cr) and HMTA-BAIL@MIL-101 (Cr) under Ar atmosphere

Our research began with examine model study using different solvents such as H_2O, EtOH, H_2O/EtOH (1:1), DMF, CH_3CN, and also under solvent-free conditions at varying temperatures. As shown in Table 1, with the increasing temperature from the 25 to 100 °C under solvent-free conditions led to an increase in the product yield within reducing reaction time and the best outcomes were achieved at 80 °C (Table 1, entry 8). Then, to have a comparison between solvent-free conditions and the presence of various solvents, the synthesis of hexahydroquinoline **5c** was carried out in the presence of HMTA-BAIL@MIL-101(Cr) (0.008 g) as catalyst under reflux conditions. Finally, the solvent-free condition was selected because it demonstrated the surprising results of these experiments involve a higher yield in short reaction time in comparison with other conditions.

To find the optimum amount of the nanocatalyst, the model reaction was accomplished by using catalyst amounts from 0 to 0.008 g. It was illustrated that the yield was increased with the addition of HMTA-BAIL@MIL-101(Cr) quantity and no

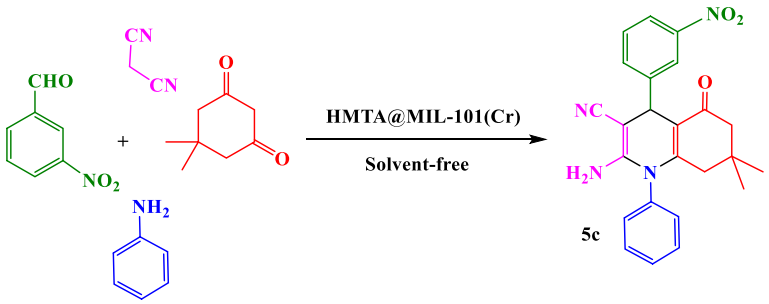

Scheme 5 Model reaction for the synthesis of 2-amino-7,7-dimethyl-4-(3-nitrophenyl)-5-oxo-1-phenyl-1,4,5,6,7,8-hexahydroquinoline-3-carbonitrile (5c)

Table 1 The optimization of various temperatures and solvents in the model reactions by using 0.008 g of HMTA-BAIL@MIL-101(Cr) as nanocatalyst

Entry	Solvent	Temp. (°C)	Time (min)	Yield[a] (%)
1	–	25	120	65
2	–	60	20	93
3	–	**80**	**10**	**98**
4	–	100	10	98
5	EtOH	Reflux	90	70
6	H_2O/EtOH	Reflux	100	65
7	H_2O	Reflux	110	31
8	DMF	Reflux	120	70
9	CH_3CN	Reflux	130	75

Bold values emphasise the best reaction conditions considering reaction time and yield of corresponding product

[a]Isolated Yield

product was obtained in the absence of the catalyst. Besides, the optimal amount of catalyst was 0.008 g with 98% yield after 10 min (Fig. 7). Moreover, with the increasing amount of the catalyst over 0.008 g no significant result was obtained.

To evaluate the catalytic efficiency of the HMTA-BAIL@MIL-101(Cr) in the synthesis of hexahydroquinoline **5c**, the model reaction was performed in the absence of catalyst and also using various catalysts including HMTA, CuI, MgO, MIL-101(Cr), ZnO and HMTA-BAIL@MIL-101(Cr) (Fig. 8). As shown in Fig. 8, a trace amount of the desired product was obtained in the absence of a catalyst. Furthermore, the summarized results from Fig. 8 demonstrated that the HMTA-BAIL@MIL-101(Cr) was afforded the product in higher yield within a shorter reaction time in comparison with other catalysts.

After optimization of the reaction conditions, we considered the synthesis of hexahydroquinoline derivatives using various aldehydes and aniline derivatives in the presence of 0.008 g of HMTA-BAIL@MIL-101(Cr) as catalyst at 80 °C under

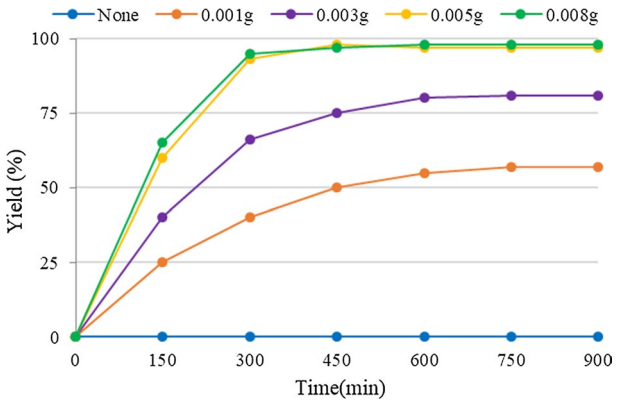

Fig. 7 The optimization of catalyst amount for the synthesis of hexahydroquinoline 5c

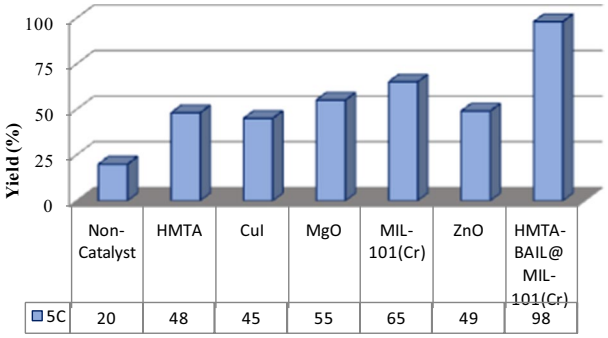

Fig. 8 The effect of various catalysts and absence of a catalyst on the model reaction

solvent-free conditions (Table 2). As expected, the aldehydes bearing electron-withdrawing groups lead to products with higher yields and shorter reaction time than those with electron-donating groups.

To show the eligibility of HMTA-BAIL@MIL-101(Cr) in the synthesis of hexahydroquinoline derivatives, we compared the presented method with some recently published works. As shown in Table 3, the advantages of this research which make it exclusiveness than other previously reported procedures, are clear reaction conditions, high yield of products with high purity, short reaction time and reusability of the catalyst for six times without considerable loss of catalytic activity.

Recycling and reusing of the catalyst

To continue, the reusability of the HMTA-BAIL@MIL-101(Cr) composite was studied under optimized reaction conditions. After completion of the reaction, the heterogeneous catalyst was dissolved in acetone and then the insoluble HMTA-BAIL@MIL-101(Cr) was separated by simple filtration. As shown in Fig. 9, the HMTA-BAIL@MIL-101(Cr) nanocatalyst could be used for six cycles whit a slightly decreased in its activity from the first run to the sixth (98–90%). The chemical structure of recovered HMTA-BAIL@MIL-101(Cr) was verified using XRD pattern and FT-IR spectrum. There is no significant difference between the XRD and FT-IR of the fresh and recovered nanocomposite (Fig. 10). Also, the acid sites (1.23 mmol/g) of the catalyst after 6 times reused had no dramatic changes based on the acid–base titration measurement, in comparison with acid sites of the fresh HMTA-BAIL@MIL-101(Cr) nanocomposite (1.26 mmol/g). These facts prove that the efficiency, appearance and structure of HMTA-BAIL@MIL-101(Cr) catalyst remained intact in recycles and there was no considerable deformation or leaching after 6 runs.

The proposed reaction mechanism

A plausible mechanism for the synthesis of hexahydroquinoline derivatives (5a-5n) catalyzed by HMTA-BAIL@MIL-101(Cr) is shown in Scheme 6. It is presumed that HMTA-BAIL@MIL-101(Cr) acts as Brønsted acid which increases

Table 2 Synthesis of hexahydroquinoline derivatives (5) using HMTA-BAIL@MIL-101(Cr) as catalyst

Entry	ArCHO	$ArNH_2$	Product	Time (min)	Yield (%)[b]	m. p. (°C)	Lit. m.p. (°C)
5a			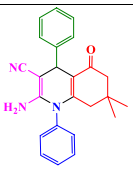	15	95	242-244	244-245[35]
5b	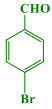		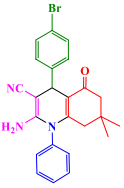	12	96	268-269	269-271[36]
5c			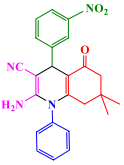	10	98	265-267	265-267[37]
5d	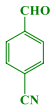		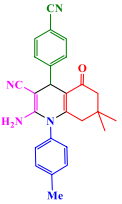	12	97	241-242	New
5e	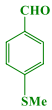		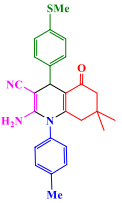	20	95	255-257	New
5f		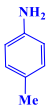	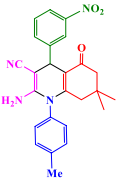	10	96	277-279	279-280[48]
5g	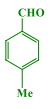	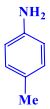	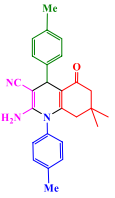	15	94	248-250	250-252[34]

Table 2 (continued)

Entry	ArCHO	$ArNH_2$	Product	Time (min)	Yield (%)[b]	m. p. (°C)	Lit. m.p. (°C)
5h	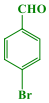	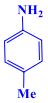	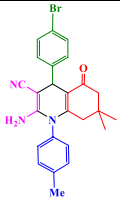	10	96	257-259	259-261[48]
5i	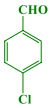	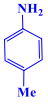	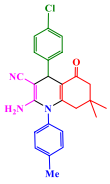	10	98	256-258	258-260[48]
5j	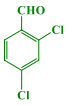		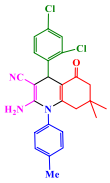	10	95	265-267	267-269[49]
5k	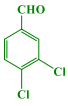	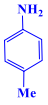	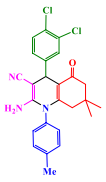	10	92	267-269	269-271[34]
5l		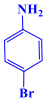	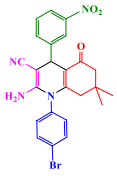	15	94	271-273	271-272[34]
5m	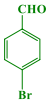		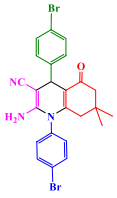	15	97	274-276	275-276[34]
5n	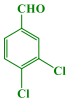	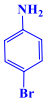	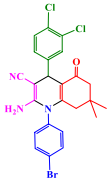	10	93	277-279	279-281[34]

Table 3 Comparison of the catalytic efficiency of HMTA-BAIL@MIL-101 (Cr) with other catalysts for the synthesis of (5c)[a]

Entry	Catalyst	Conditions	Time (min)	Yield (%)[b]	TON[c]
1	MNP@BSAT@Cu(OAc)$_2$	EtOH/reflux	14	83 [37]	93
2	Zr(HPO$_4$)$_2$	Solvent-free, (80 °C)	120	97 [34]	86
3	DBU (5 mol %)	MW/EtOH, (90 °C)	4	96 [48]	63
4	[bmim$^+$][BF$^-_4$]	90 °C	5	96 [49]	450
5	HMTA-BAIL@MIL-101(Cr)	Solvent-free, (80 °C)	10	98	138

[a]Based on the multicomponent reaction of 3-nitrobenzaldehyde, malononitrile, dimedone and aniline.
[b]Isolated yield

[c]*TON* turnover number (mol of the product/mol of the catalyst)

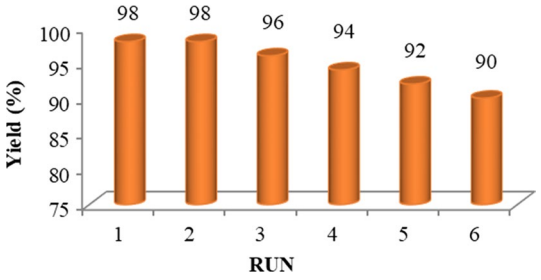

Fig. 9 Reusability of HMTA-BAIL@MIL-101(Cr) catalyst

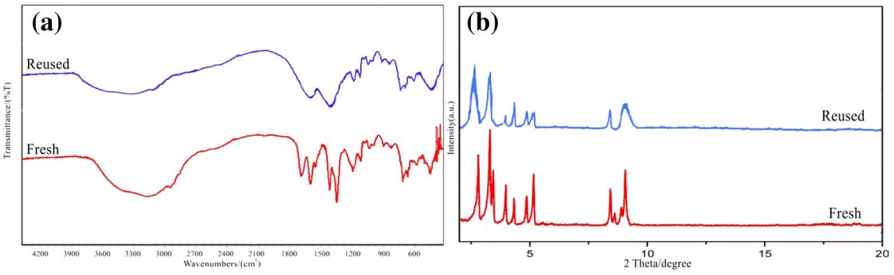

Fig. 10 FT-IR spectrum (**a**) and XRD pattern (**b**) of the recovered HMTA-BAIL@MIL-101(Cr) after 6 runs

the electrophilicity of the carbonyl groups of the dimedone and aldehyde through a strong coordination bond [34]. Initially, malononitrile reacts with aromatic aldehyde catalyzed by the HMTA-BAIL@MIL-101(Cr) through a Knoevenagel condensation to generate intermediate **I**. After that, the formation of intermediate **III** occurred from Michael-type addition of enamine **II**, which is obtained from the reaction of dimedone and arylamine to intermediate **I** in the presence of nanocatalyst. The intermediate **III** undergoes intramolecular cyclization and

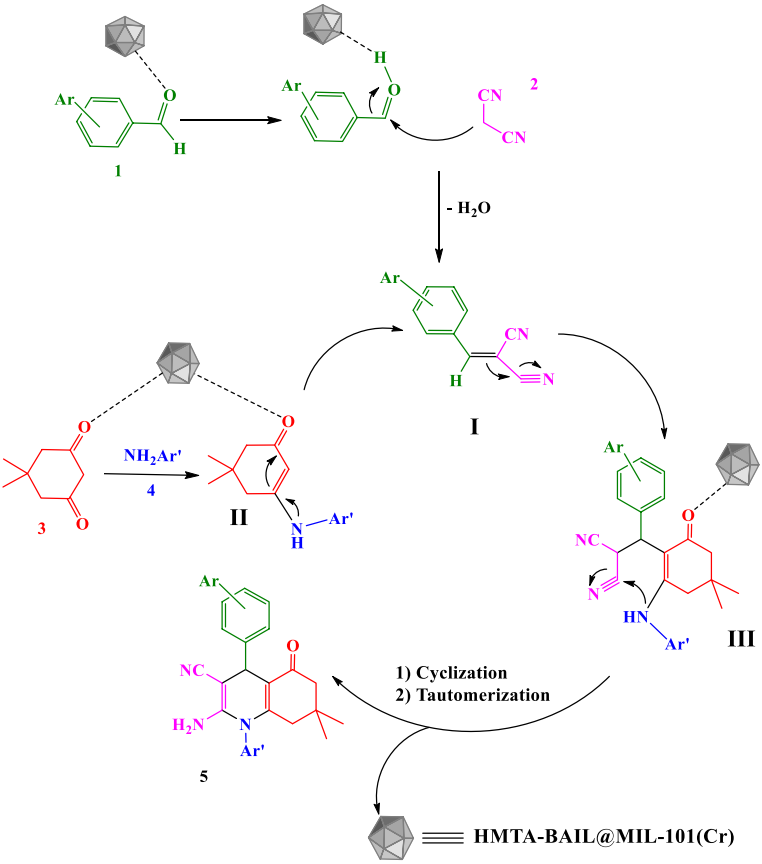

Scheme 6 Proposed mechanism for the synthesis of hexahydroquinoline derivatives using HMTA-BAIL @MIL-101(Cr)

tautomerization using HMTA-BAIL@MIL-101(Cr) catalyst to form the desired hexahydroquinoline derivatives in high yield and short reaction time.

Conclusion

In summary, we have designed an efficient and robust heterogeneous catalyst including HMTA-BAIL@MIL-101(Cr) for the one-pot synthesis of hexahydroquinoline derivatives via the reaction of aromatic aldehydes, aryl amines, malononitrile and dimedone under solvent-free conditions. This new catalyst was easily recovered and reused for six cycles without a significant loss of its catalytic activity. The characterization of the prepared heterogeneous catalyst was carried out by various spectroscopy techniques like SEM, XRD, EDS, TGA, BET and FT-IR analysis. It is notable that the procedure has shown diverse advantages, such as excellent yields of

the preparation hexahydroquinolines, short reaction times, environmentally process, reusability of the catalyst and low catalyst loading. Consequently, the presented method provides a green and effective method for the synthesis of hexahydroquinolines under mild reaction conditions.

Acknowledgements The authors gratefully acknowledge the financial support of this work by the Research Affairs Office of the Islamic Azad University, Qom Branch, Qom, I. R. Iran [Grant Number 2019-2898].

References

1. Z. Hong-Cai, J.R. Long, O.M. Yaghi, Chem. Rev. **112**, 673 (2012)
2. M.A. Ghasemzadeh, B. Mirhosseini-Eshkevari, M. Tavakoli, F. Zamani, Green Chem. **22**, 7265 (2020)
3. H. Shayegan, A.M. Ali Gomaa, V. Safarifard, ChemistrySelect **5**, 124 (2020)
4. M. Eddaoudi, J. Kim, N. Rosi, D. Vodak, J. Wachter, M. O'Keefe, O.M. Yaghi, Science **295**, 469 (2002)
5. T.R. Cook, Y.R. Zheng, P.J. Stang, Chem. Rev. **113**, 734 (2013)
6. A. AzhdariTehrani, H. Ghasempour, A. Morsali, G. Makhloui, C. Janiak, Cryst. Growth Des. **15**, 5543 (2015)
7. H. Ghasempour, A.A. Tehrani, A. Morsali, J. Wang, P.C. Junk, CrystEngComm **18**, 2463 (2016)
8. A.A. Tehrani, S. Abedi, A. Morsali, J. Wang, P.C. Junk, J. Mater. Chem. A. **3**, 20408 (2015)
9. S. Qiu, M. Xue, G. Zhu, Chem. Soc. Rev. **43**, 6116 (2014)
10. Q.X. Luo, B.W. An, M. Ji, J. Zhang, Mater. Chem. Front. **2**, 219 (2018)
11. Y. Takashima, M. Yokoyama, A. Horikoshi, Y. Sato, T. Tsuruoka, K. Akamatsu, New J. Chem. **41**, 14409 (2017)
12. D. Farrusseng, S. Aguado, C. Pinel, Angew. Chem. Int. Ed. **48**, 7502 (2009)
13. L. Jiao, J.Y.R. Seow, W.S. Skinner, Z.U. Wang, H.-L. Jiang, Mater. Today. **27**, 43 (2019)
14. A. Dhakshinamoorthy, A.M. Asiri, M. Alvaro, H. Garcia, Green Chem. **20**, 86 (2018)
15. A. Dhakshinamoorthy, H. Garcia, Chem. Soc. Rev. **43**, 5750 (2014)
16. A. Dhakshinamoorthy, A.M. Asiri, H. García, Trends Chem. **2**, 454 (2020)
17. A. Dhakshinamoorthy, A. Santiago-Portillo, A.M. Asiri, H. Garcia, ChemCatChem. **11**, 899 (2019)
18. T. Welton, Chem. Rev. **99**, 2071 (1999)
19. D.B. Zhao, M. Wu, Y. Kou, E.Z. Min, Catal. Today. **74**, 157 (2002)
20. P. Wasserscheid, M. Sesing, W. Korth, Green Chem. **4**, 134 (2002)
21. G. Aridoss, K.K. Laali, J. Org. Chem. **76**, 8088 (2011)
22. J.K. Park, P. Sreekanth, B.M. Kim, Adv. Synth. Catal. **346**, 49 (2004)
23. B.C. Ranu, S. Banerjee, R. Jana, Tetrahedron **63**, 776 (2007)
24. F.G. Zanin, A. Macedo, M. Archilha, E.P. Wendler, A.A. Dos Santos, Bioresour. Technol. **143**, 126 (2013)
25. Y.A. Elsheikh, Ind. Crops Prod. **49**, 822 (2013)
26. F. Han, L. Yang, Z. Li, C.G. Xia, Adv. Synth. Catal. **354**, 1052 (2012)
27. A.S. Amarasekara, B. Wiredu, Ind. Eng. Chem. Res. **50**, 12276 (2011)
28. A. Domling, I. Ugi, Angew. Chem. Int. Ed. **39**, 3168 (2000)
29. A. Ryckebusch, R. Derprez-Poulain, L. Maes, M.A. Debreu-Fontaine, E. Mouray, P. Grellier, C. Sergheraert, J. Med. Chem. **46**, 542 (2003)
30. L.R. Morgan, B.S. Jursic, C.L. Hooper, D.M. Neumann, K. Thangaraj, B. Leblanc, Bioorg. Med. Chem. Lett. **12**, 3407 (2002)
31. N. Fokialakis, P. Magiatis, L. Chinou, S. Mitaku, F. Tillequin, Chem. Pharm. Bull. **50**, 413 (2002)
32. P. Fossa, L. Mosti, G. Menozzi, C. Marzano, F. Baccichetti, F. Bordin, Bioorg. Med. Chem. **10**, 743 (2002)
33. P. Beagley, M.A.L. Blackie, K. Chibale, C. Clarkson, R. Meijboom, J.R. Moss, P. Smith, H. Su, Dalton Trans. **15**, 3046 (2003)

34. S. Abdolmohammadi, Z. Naturforsch, Zeitschrift für Naturforschung B. **68**, 195 (2013)
35. M. Abaszadeh, M. Seifi, J. Sulfur Chem. **38**, 440 (2017)
36. B. Amirheidari, M. Seifi, M. Abaszadeh, Res. Chem. Intermed. **42**, 3413 (2016)
37. N. Ahadi, A. Mobinikhaledi, M.A. Bodaghifard, Appl. Organometal. Chem. **34**, e5822 (2020)
38. M.A. Ghasemzadeh, B. Mirhosseini-Eshkevari, M.H. Abdollahi-Basr, Appl. Organometal. Chem. **33**, 4679 (2018)
39. M.A. Ghasemzadeh, M. Azimi-Nasrabad, S. Farhadi, B. Mirhosseini-Eshkevari, J. Organomet. Chem. **900**, 120935 (2019)
40. H. Saeidiroshan, L. Moradi, J. Organomet. Chem. **893**, 1 (2019)
41. J. Safari, M. Tavakoli, M.A. Ghasemzadeh, Polyhedron **182**, 114459 (2020)
42. M.A. Ghasemzadeh, B. Mirhosseini-Eshkevari, M.H. Abdollahi-Basir, Appl. Organometal. Chem. **33**, 4679 (2018)
43. J. Zhang, S. Bao, J. Yang, Chin. Sci. Bull. **54**, 3958 (2009)
44. C. Férey, C. Mellot-Draznieks, F. Serre, J. Millange, S.S. Dutour, I.A. Margiolaki, Science **309**, 2040 (2005)
45. C.P. Cabello, G. Berlier, G. Magnacca, P. Rumori, G.T. Palomino, Cryst. Eng. Commun. **17**, 430 (2015)
46. H. Wei, B. Teo, A. Chakraborty, S. Kayal, Appl. Therm. Eng. **101**, 891 (2016)
47. T. Hu, Q. Jia, S. He, S. Shan, H. Su, Y. Zhi, L. He, J. Alloys Compd. **727**, 114 (2017)
48. S.K. Singh, K.N. Singh, Monatsh. Chem. **143**, 805 (2012)
49. X.S. Wang, M.M. Zhang, H. Jiang, C.S. Yao, S.J. Tu, Tetrahedron **63**, 4439 (2007)